# Effective Propagation of HPAM Solutions Through the Tambaredjo Reservoir During a Polymer Flood

**R.N. Manichand,** SPE, and **K.P. Moe Soe Let,** SPE, Staatsolie Maatschappij Suriname N.V.; **L. Gil,** SPE, and **B. Quillien,** SNF SAS; and **R.S. Seright,** SPE, New Mexico Institute of Mining and Technology

## Summary

Two new methods were developed for anaerobically sampling polymer solutions from production wells in the Sarah Maria polymer-flood-pilot project in Suriname. Whereas previous methods indicated severe polymer degradation, the improved methods revealed that the polymer propagated intact more than 300 ft through the Tambaredjo formation. Our results may help explain the inconsistency between good production responses and highly degraded polymer observed in many past field projects. Analysis of produced salinity, polymer concentration, and viscosity indicated that the polymer banks retained low salinity and, therefore, high viscosity for much of the way through the Sarah Maria polymer-flood-pilot pattern. A strong shear-thickening rheology was observed for 1,000 ppm and 1,350 ppm hydrolyzed polyacrylamide (HPAM) solutions in porous media, even though the salinity was only 500 ppm total dissolved solids (TDS). Examination of injectivities revealed that these solutions were injected above the formation parting pressure in the Sarah Maria polymer-injection wells. Injectivity was insufficient until fractures were initiated hydraulically; however, the fractures propagated a distance of only approximately 20 ft and did not jeopardize sweep efficiency. In contrast, the short fractures greatly improved polymer injectivity and reduced concern about polymer mechanical degradation.

## Introduction

In polymer floods and other chemical floods that use water-soluble polymers for mobility control, the polymer should remain stable for most of its transit through the reservoir to maintain sufficient viscosity to efficiently displace oil. However, for many cases in which polymer samples were collected from production wells, the polymer was severely degraded, even in low-temperature applications. Extensive sampling of production wells at Daqing revealed approximately 80% loss of viscosifying ability for HPAM after travelling approximately 800 ft through the Daqing sand at 45°C (Zhang 1995; Wang et al. 2006). After a residence time of 2 to 3 years in the Daqing reservoir, You et al. (2007) reported that polymer molecular weight decreased by 92% (from 19.8 million daltons to 0.89 million daltons), and the degree of hydrolysis increased by approximately 29% (from 28 to 36.2%). You et al. (2007) also reported that after transiting the Shengli reservoir (70°C, 2- to 3-year residence time), HPAM molecular weight decreased by 77.2% (from 17.3 million daltons to 3.94 million daltons), and the degree of hydrolysis increased by 71.5% (from 22.3 to 38.2%). After transiting the Shuanghe (Henan) reservoir (70°C, 2- to 4-year residence time), You et al. (2007) reported HPAM molecular weight decreased by 84.6% (from 15.2 million daltons to 2.35 million daltons), and the degree of hydrolysis increased by 151% (from 23.7 to 59.5%). Putz et al. (1994) examined HPAM produced from the Courtenay polymer flood (30°C). After transiting approximately 500 ft through the formation, the HPAM lost approximately half of its viscosifying ability. As will be described in the present paper, during our first testing procedures for solutions produced from the Sarah Maria polymer pilot in the Tambaredjo field (Suriname), we also observed that HPAM experienced a substantial (83%) drop in molecular weight upon transiting approximately 330 ft through the formation at 38°C.

The preceding observations are disturbing since they raise questions about when and how polymer degradation occurred. If degradation occurred during or shortly after injection, the viability of the polymer flood should be seriously jeopardized. In contrast, if degradation occurred at or near the production wells, the degradation has little/no negative impact. On a positive note, these polymer floods exhibited very positive oil-production responses. Nevertheless, because polymer costs represent a substantial part of the investment during a polymer flood, understanding where and how polymer degradation occurs can have considerable value. Previous laboratory work indicated that HPAM solutions should be quite stable at low temperatures, considering the conditions present in most low-temperature reservoirs (Shupe 1981; Yang and Treiber 1985; Moradi-Araghi and Doe 1987; Seright et al. 2010). So, why was severe degradation observed in the aforementioned field projects?

In this paper, we test a hypothesis that the polymer degradation occurred dominantly during the time between polymer production from the well and viscosity measurement. More specifically, our hypothesis is that when polymer solutions (even with high oxygen content) are injected into a reservoir, pyrite ($FeS_2$), siderite ($FeCO_3$), and other iron ($Fe^{2+}$) minerals rapidly reduce the dissolved oxygen content to undetectable levels within a few days, even at low temperatures. In this reduced condition, $Fe^{2+}$ can readily dissolve into the polymer solution (at a level of 0.2 to 1.2 ppm in our specific case). This iron has no effect on the polymer as long as no free oxygen or oxidizing agent is present—so the polymer provides effective viscosity (Seright et al. 2010). However, once the polymer solution is produced and mixed with oxygen, the polymer can rapidly degrade.

We developed a simple sampling arrangement/procedure that allows collection of polymer samples from a well, introduction into a Brookfield viscometer, and viscosity measurement—all under anaerobic conditions. We also applied a second method, in which 10 $cm^3$ of a stabilizing solution containing specific sacrificial agents and radical scavengers was mixed with the collected sample to proactively counter any iron-induced oxidative degradation that may occur when the sample is exposed to atmospheric conditions during measurements. Using these methods, we demonstrate that the HPAM polymer is transported approximately 330 ft through the Tambaredjo reservoir with no loss of viscosifying ability. Without using these procedures, produced-polymer samples lost more than 75% of their viscosifying ability within an hour of collection. This paper describes the sampling procedures, and examines the effective injection and propagation of HPAM solutions in the Sarah Maria polymer-flood pilot.

## The Sarah Maria Polymer-Flood Pilot

**Reservoir Description.** Staatsolie's Sarah Maria polymer-flooding-pilot project in the Tambaredjo field **(Fig. 1)** currently has

---

This paper (SPE 164121) was accepted for presentation at the SPE International Symposium on Oilfield Chemistry, The Woodlands, Texas, USA, 8–10 April 2013, and revised for publication. Original manuscript received for review 21 December 2012. Revised manuscript received for review 29 April 2013. Paper peer approved 2 May 2013.

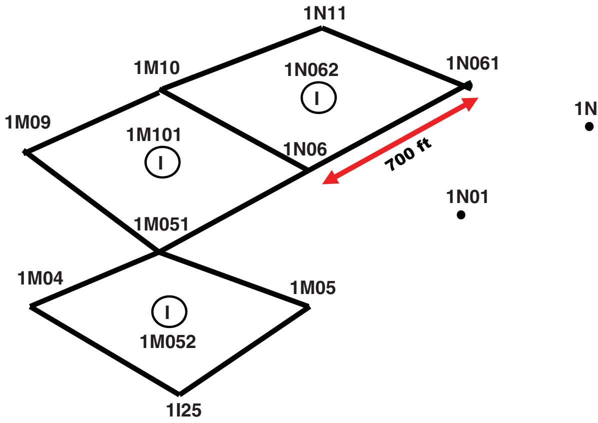

**Fig. 1—Sarah Maria polymer-pilot project.**

three injection wells (1M101, 1N062, and 1M052) with nine offset production wells (1M09, 1M10, 1N06, 1M051, 1N11, 1N061, 1M04, 1M05, and 1I25). Solution-gas drive and compaction were largely responsible for the 20%-of-original-oil-in-place (OOIP) recovery factor associated with primary recovery in the pilot area. No active waterdrive in this part of the field is evident, and no waterflood has been implemented. A combination of rock-and-fluid expansion and reservoir compaction (associated with decreased pore pressure) appears to be responsible for most formation water produced from the project area. Average permeabilities for the T1 sand (the main productive interval) range from 4 to 12 darcies. A significant level of heterogeneity exists in the Tambaredjo reservoir, with a 12:1 permeability contrast observed for the approximately 20-ft-thick T1 layer and the overlying 15-ft-thick T2 layer. No significant flow barriers exist between the two layers. To supplement the compaction- and solution-gas-drive mechanisms, polymer injection is being evaluated. High oil viscosity in the Tambaredjo field mandates that polymer injection is preferred over water injection. Produced oils range in viscosity from 1,260 to 3,057 cp, with an average of 1,728 cp. Water viscosity at reservoir temperature (100°F, 38°C) is approximately 0.7 cp.

**Polymer Injection and Breakthrough.** Polymer injection into Well 1M101 began in September 2008. Injection rate varied between 160 and 335 B/D (September 2008–August 2012). As of August 2012, 335,679 bbl of polymer solution had been injected into Well 1M101. Polymer injection into Well 1N062 began in May 2010 and has continued with rates between 220 and 320 B/D. As of August 2012, 236,575 bbl of polymer solution had been injected into Well 1N062. Polymer injection in a third well, 1M052, began in June 2011. As of August 2012, 99,574 bbl had been injected into this well at rates varying between 150 and 270 B/D. Considering the pore volume (PV) of all three injection patterns, approximately 24% PV of polymer solution had been injected as of August 2012. Oil and water-cut responses to polymer injection and results from interwell tracer studies can be found in Moe Soe Let et al. (2012).

Polymer breakthrough was modest and gradual in the first injection pattern, being detected in the producers located west and north of the injector. In the second injection pattern, the polymer breakthrough was more evident, and higher concentrations of polymer were produced quickly in wells in the north/south direction. In the third injection pattern, polymer breakthrough also was observed in the wells south of the injector. Well 1N11 is currently producing a polymer concentration that is 66% of the 1,350-ppm injected concentration. Three wells (1N01, 1N06, and 1I25) are producing 34–41% of the injected polymer concentration. Two wells (1M05 and 1M09) are producing 16–21% of the injected polymer concentration. Six other wells are producing small (less than 5%) but detectable polymer concentrations. On the basis of the polymer-breakthrough times and concentrations, the level of channeling is significantly greater in the second injection pattern.

**Water Quality and Polymer Mixing.** The water used for mixing polymer solutions was clear, with no sign of particulates. Polymer-solution concentrate was also clear and well-dissolved. Polymer preparation and water quality were uniform, reliable, and consistent, with only occasional upsets. Until November 2011, prepared polymer solutions contained 1,000-ppm SNF Flopaam 3630S HPAM (molecular weight ≈ 18 million daltons) in approximately 400- to 500-ppm-TDS Sarah Maria water and consistently had a viscosity of approximately 50 cp (at ambient temperature and 7.3 $s^{-1}$) at the mixing facility and approximately 45 cp at the closest injection well (1M101). Since November 2011, the injected polymer concentration was raised to 1,350 ppm—providing a viscosity of approximately 85 cp (at 7.3 $s^{-1}$).

At the Sarah Maria polymer project, the salinity of the injected polymer solutions is 400–500 ppm TDS, but the formation water typically has ten times greater salinity. HPAM polymers are extremely effective viscosifiers at low salinities, but they lose much of their effectiveness as salinity is increased. We expect the Sarah Maria polymer solution to lose more than half of its original viscosity if mixing with the formation water increased the salinity to approximately 4,700 ppm TDS. This type of mixing is most likely to occur if the mobility ratio is high, as at the Sarah Maria project. The mixing occurs because thin viscous fingers penetrate through the formation, so the saline formation water does not have to travel far (by diffusion or dispersion) to mix with the polymer water. As the viscosity of the polymer water is increased, this mixing effect is reduced. So, an incentive exists to inject the most-viscous polymer solution that is practical. This concept was demonstrated effectively in German polymer floods in which freshwater polymer solutions were injected into formations with 17%-TDS brines (Maitin 1992).

**Salinity Response.** The salinity of the water in the injected-polymer solutions was considerably less (400–500 ppm TDS) than in the formation water (2,500–5,000 ppm TDS). Thus, salinity of the produced water may reflect breakthrough from injection wells. **Fig. 2** plots salinity of the water from the pilot's production wells. The largest and most abrupt salinity drop occurred in Well 1N11—the north well in the second polymer pattern. The response started approximately 1 month after the start of polymer injection (into Well 1N062). Most of the salinity decrease occurred over a 5-month period, eventually leveling off at one-quarter of the original salinity (but still approximately three times the salinity of the injected water).

Relatively quick salinity responses were also seen in Wells 1N06 and 1I25. The responses in Wells 1N11 and 1N06 indicate a north/south channel through Injector 1N062. The response in Well 1I25 suggests a north/south channel through Injector 1M052. Gradual salinity declines were noted in Wells 1M09, 1M10, 1N061, and 1M05. No significant salinity change has been noted yet in Wells 1M04 and 1M051. These results indicate that the first polymer pattern shows no sign of channeling in any direction. They also suggest that channeling does not occur in the east/west direction in any of the three patterns.

## First Tests of Polymer Stability

Our expectation was that the HPAM polymer would be quite stable under the conditions experienced at the Sarah Maria pilot site. The temperature was low—only 100°F (38°C) in the reservoir, so no oxidative degradation was anticipated unless a redox couple was established. However, two pieces of information caused concern. The first was that dissolved oxygen levels were ambient (3–8 ppm) throughout the mixing and injection process. The second piece of information that raised concern was from a polymer-backflow test that was conducted from October to November of 2009. Although the injected-polymer samples had viscosities ranging from 40 to 45 cp, viscosities were noticeably less for samples backflowed from Well 1M101. Most disturbing, an analysis indicated that the backflow samples had polymer molecular weights reduced from the original 18 million daltons to only 3 million daltons.

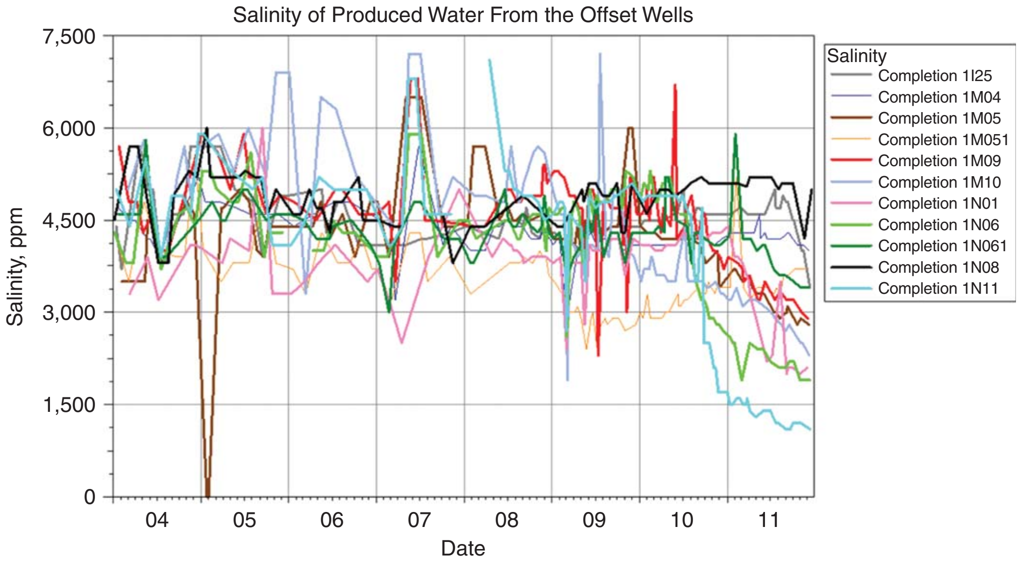

**Fig. 2—Salinity responses in production wells during the polymer flood.**

Three additional tests were performed in 2010, 2011, and 2012, during which produced-polymer samples were typically collected in a sample bomb **(Fig. 3).** These samples were shipped to France for analysis, including polymer concentration, anionicity, intrinsic viscosity, and molecular weight. Samples were dialyzed to correct for salinity. Intrinsic viscosity measurements were performed by use of capillary tubes at 30°C in 1 M NaCl, pH=7. **Table 1** summarizes the results from these tests. Except for those samples indicated in Table 1, all samples were collected using the sample bomb—at the time, it was presumed under anaerobic conditions. Examination of Table 1 reveals two central points. The first is that the anionicity of the produced samples was unchanged compared with that of the injected polymer. This result was expected because the temperature was low and pH was near neutral (Moradi-Araghi and Doe 1987). The second, and most important, point was that in all cases, the molecular weight of the produced polymer was 4 to 22% of that of the injected polymer. Further, the samples collected with the sample bomb (supposedly anaerobic) showed the same level of degradation as those collected aerobically without the sample bomb. If accepted, this result would be of major concern. Consequently, improved sampling and measurement methods should be investigated.

**Fig. 3—Sample cylinder for polymer collection.**

## Improved On-Site-Sampling and -Measurement Methods

We suspected that the preceding negative results for polymer stability occurred because oxygen was mixed with polymer solution having significant iron content before measurement of polymer properties. Polymer solutions can tolerate high dissolved $Fe^{2+}$ concentrations, as long as no free oxygen is present (Shupe 1981; Yang and Treiber 1985; Seright et al. 2010). If free oxygen is introduced, a redox reaction will be initiated that degrades the HPAM polymer. When the polymer solution was injected at Sarah Maria, it contained little or no dissolved iron, but it contained 3–8 ppm dissolved oxygen. However, on the basis of literature reports and analysis (Seright et al. 2010), within days of injection, iron minerals in the formation remove all this dissolved oxygen. In the process, $Fe^{2+}$ was introduced into the polymer solution (0.2–1.2 ppm $Fe^{2+}$, from our measurements of produced samples). Presumably, the polymer flowed intact through the reservoir, effectively improving sweep efficiency. After arriving at the producer, introduction of free oxygen during or after sampling caused severe polymer degradation.

**First Improved Sampling Method.** To test the preceding concept, we collected an anaerobic sample from Well 1N11. Fig. 3 shows the sample apparatus. During sample collection, it was very important to point the bottom end of the cylinder upward, so that gas was displaced and the cylinder was able to fill completely with liquid. If the cylinder was filled with the bottom end pointed downward (as occurred during previous sampling), a large pocket of air remained. Oxygen in this air could degrade the polymer. After allowing the sample to settle overnight to allow oil to float to the top of the cylinder, we connected the sample cylinder to a special set of fittings that allowed anaerobic liquid to flow directly from the sample cylinder into the bottom of the Brookfield viscometer's UL adapter and out of the top of the UL adapter **(Figs. 4 and 5).** Just after the outlet valve of the sample cylinder, we placed a 6-inch tube section that contained a rolled paper towel to filter any oil. Although we had a nitrogen cylinder (with 300-psi nitrogen) ready to drive polymer solution from the sample cylinder into the UL adapter, it was not needed because the sample cylinder was sufficiently pressurized during collection at the wellhead.

After filling the UL adapter with polymer solution, the valve at the end (bottom) of the sample cylinder was closed and the

TABLE 1—RESULTS FOR SAMPLES THAT WERE SHIPPED TO FRANCE FOR ANALYSIS*

| Sample | Polymer Concentration (ppm) | Anionicity (%) | Intrinsic Viscosity (mL/g) | Molecular Weight ($10^6$ daltons) |
|---|---|---|---|---|
| First series, 2010 | | | | |
| 1M101 Sample #OB | 435 | 31.3 | 5.40 | 2.01 |
| 1M101 Sample #4 | 620 | 32.1 | 6.92 | 2.93 |
| 1M101 Sample #22 | 615 | 31.9 | 8.56 | 4.04 |
| Second series, 2011 | | | | |
| 1N11 with sample bomb | 450 | 30.0 | – | – |
| 1N11 no sample bomb | 454 | 29.4 | 4.31 | 1.43 |
| 1M09 | 70 | 26.6 | 3.73 | 1.15 |
| 1N06 | 244 | 29.4 | 4.40 | 1.48 |
| 1M05 | 72 | 23.5 | 3.09 | 0.86 |
| 1M10 | 15 | 28.5 | – | – |
| Third series, 2012** | | | | |
| 1M09 | 140 | 26.2 | 4.79 | 1.68 |
| 1I25 | 320 | 31.2 | 7.13 | 3.07 |
| 1N11 with sample bomb | 580 | 31.4 | 5.57 | 2.11 |
| 1N11 without sample bomb | 550 | 32.4 | 6.02 | 2.37 |

* Initial polymer molecular weight: 18 million daltons. Initial anionicity: ≈30%.
** pH values all measured between 6.5 and 6.9. Results after ultrafiltration.

viscometer motor was turned on—measuring viscosities from 31 to 34 cp, during several sampling periods. Dissolved oxygen was measured for the fluid that came out from the top of the UL adapter—revealing 10–15 ppb dissolved oxygen. Dissolved iron was measured at 0.2 ppm, and salinity was measured at 1600 ppm TDS. For comparison, an oxygenated polymer solution was collected from 1N11. Within an hour of collection, viscosity was measured at 7.3 $s^{-1}$ (i.e., 6 rev/min) and found to be 6 cp. Thus, less than one hour of contact with dissolved oxygen caused substantial viscosity loss (i.e., from 31 to 34 cp down to 6 cp) for the polymer solution with 0.2 ppm dissolved iron.

The polymer concentration produced from Well 1N11 contained 896 ppm HPAM. Separate measurements revealed that a freshly prepared solution of 900 ppm HPAM in 1600-ppm-TDS brine should provide a viscosity of at least 20 cp (at 7.3 $s^{-1}$ and 25°C). Our measured viscosity for the produced polymer fluid (31–34 cp) indicates that the polymer has propagated through the reservoir with no significant degradation. In support of this conclusion, we noted long, thin liquid strings at the last stage of pouring the produced-polymer solutions from a container. This stringiness is caused by very-high-molecular-weight polymers. (In contrast, polymer-free solutions show discrete drops during this procedure.) These very-high-molecular-weight polymers are the most likely species to be destroyed or removed by mechanical degradation, oxidative degradation, and retention within the porous media. Because these polymers were propagated approximately 330 ft through the formation from Injector 1N062 to Producer 1N11, we have greater confidence that the polymer was effective in providing viscosity and effective sweep in the polymer pilot. Additional measurements were made for produced-polymer samples from two other wells; **Table 2** summarizes the results.

**Second Improved Sampling Method.** For the second sampling method, the configuration shown in **Fig. 6** was used. For setup and installation of this device, we first filled a 150-$cm^3$ cylinder with 50 $cm^3$ of stabilizing chemical solution that contained sacrificial agents and radical scavengers. This cylinder was pressurized to 20–30 bar (290–435 psi) with nitrogen. Next, the cylinder was connected to Valve 3 by means of a quick coupling. After

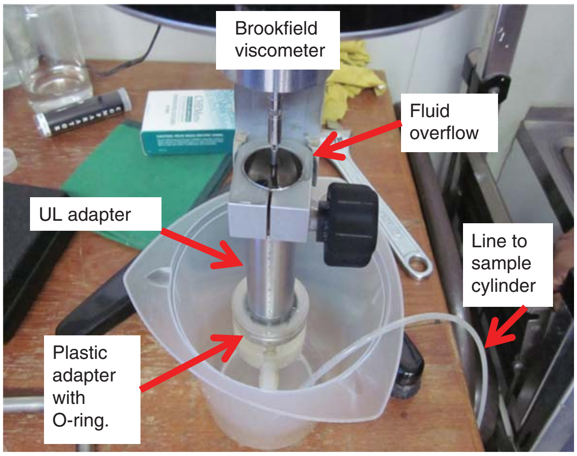

**Fig. 4—Sample-transfer arrangement showing connection to the viscometer.**

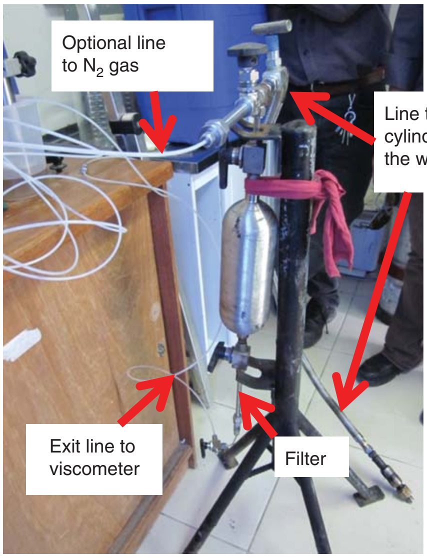

**Fig. 5—Sample-collection cylinder, ready to flow sample to the viscometer anaerobically.**

TABLE 2—SUMMARY OF MEASUREMENTS OF PRODUCED FLUIDS USING NEW SAMPLING METHOD 1

| Well | cp at 6 rev/min | Polymer (ppm) | TDS (ppm) | Fe (ppm) |
|---|---|---|---|---|
| 1N11 | 31–34 | 896 | 1,600 | 0.2 |
| 1N06 | 9.5 | 465 | 2,390 | 1.0 |
| 1M051 | 1 | 0 | 3,740 | 1.2 |

checking that all valves (in Fig. 6) were closed, the sampling system was connected to the sampling point at Valve 1. After installation, the sampling sequence was as follows:

A. Collect the sample in the 500-cm$^3$ cylinder.

1. Open Valve 1.
2. Open the three-way Valve 4 to allow flow toward Valve 5.
3. Open Valve 5 to waste. The flow can be regulated from this valve to avoid shear degradation. Flush the sampling cylinder with at least 1500 cm$^3$.
4. Close Valve 5.
5. Close Valve 1. If needed, release the pressure in the sampling cylinder slightly with Valve 5. The pressure should ultimately be slightly greater than atmospheric. For this particular field application, this step was not needed because the wellhead pressure was 3–4 bar (40–60 psi).

B. Empty the capillary tube (discharge line).

1. Open the three-way Valve 4 to the atmosphere.
2. Open Valve 5.
3. Drain to waste until empty.
4. Close Valve 5.

C. Add the stabilizing formulation.

1. Open Valve 3.
2. Open the three-way Valve 4 to waste (toward Valve 5). At this time, the addition can be sensed by touching the sampling cylinder. The capillary tube is now full of fluid, because the stabilizing chemical in the pressurized cylinder is pushed into the sampling cylinder.
3. Close Valve 3.
4. Wait for 5 minutes.

D. Fluid discharge.

1. Open Valve 5.
2. Open Valve 2. The fluid is flowing and can be collected in a sample bottle for measurement.

Several tests were performed to compare the two methods (see **Table 3**), as applied to polymer samples collected from production wells 1N11 and 1N06. The highest viscosity values (measured at 7.3 s$^{-1}$ and room temperature) were recorded using Method 1, which did not add a chemical stabilizer and which transferred the produced solution anaerobically from the sample-collection cylinder into the Brookfield viscometer. Samples collected using Method 2, but without adding stabilizer, provided higher viscosities (15 cp for 1N11 and 9 cp for 1N06) than from direct aerobic-sample collection (6 cp for 1N11). Samples collected using Method 2, with a single 10-cm$^3$ dose of stabilizer, provided even higher viscosities (19.5 cp for 1N11 and 9.5 cp for 1N06). Samples collected using Method 2, with a triple dose of stabilizer (i.e., approximately 30 cm$^3$), provided viscosities that approached those for Method 1. Dilution of polymer concentration is small (less than 6%) from addition of the stabilizer.

TABLE 3—COMPARISON OF MEASUREMENTS OF PRODUCED FLUIDS USING METHODS 1 AND 2

| Well | 1N11 | 1N06 |
|---|---|---|
| Polymer (ppm) | 896 | 465 |
| | cp at 7.3 s$^{-1}$ | |
| Direct aerobic sampling | 6 | 5 |
| Method 1 (no stabilizer) | 32 | 14 |
| Method 2, no stabilizer | 15 | 9 |
| Method 2, single dose of stabilizer | 19.5 | 9.5 |
| Method 2, triple dose of stabilizer | 30 | 12 |

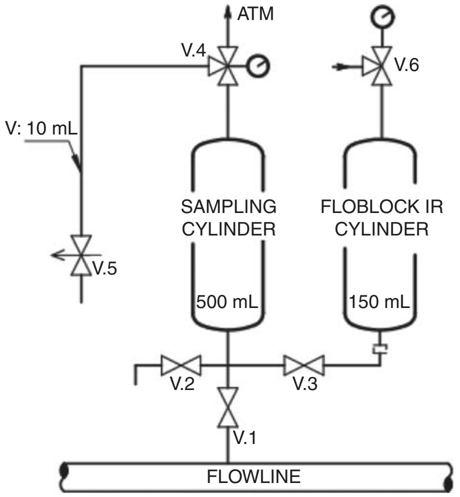

Fig. 6—Second improved-sampling method. V = valve.

Method 1 consistently provided the highest viscosities, suggesting the least polymer degradation during collection and measurement. However, this method requires a sample cylinder (Fig. 3), typically for a 24-hour period while gravity separates the oil from the water. If multiple samples are to be collected at the same time, multiple sample cylinders are needed. In contrast, Method 2 allows several samples to be collected in a short time with a single sample cylinder.

Several improvements are being incorporated into Method 2, including: (1) A pressure gauge can be installed on the cylinder containing the stabilizing chemical. Indeed, residual pressure in the cylinder aids proper chemical addition. (2) Higher chemical addition resulted in higher viscosities. A stabilizing chemical with higher/lower dosage can be formulated so that a single dosage can be applied for a given sample. (3) To avoid capillary-pipe blockage (which is detrimental to chemical addition), one pipe can be installed for flushing purposes and another pipe, with larger diameter and shorter length, can be installed for chemical addition to allow easier cleanout of oil before each sampling.

## Oxygen in the Injection Water

Ambient levels (3–8 ppm) of dissolved oxygen were present in the Sarah Maria polymer source water and in the injected polymer solutions. Fortunately, $FeS_2$ and siderite $FeCO_3$ are commonly present in reservoirs and can quickly consume any dissolved oxygen. Using a geochemical simulator, Seright et al. (2010) demonstrated that a reservoir at 25°C with 1% $FeS_2$ would reduce a solution that originally contained 5,000 ppb dissolved oxygen to less than 1 ppb $O_2$ in less than 4 days. They also performed experiments with an HPAM solution with 3,300 ppb $O_2$ that was placed in contact with anaerobic sand from the Daqing reservoir (containing 0.23% $FeS_2$ and 0.51% $FeCO_3$). Within 24 hours at 45°C, the dissolved-oxygen level was reduced from 3,300 ppb to 0 ppb, with less than 7% loss of solution viscosity. Because cores from the Sarah Maria pilot project contained up to 12% $FeS_2$/$FeCO_3$, we also expect dissolved oxygen to be removed quickly from the injected fluids. Dissolved-oxygen measurements from produced water at the Sarah Maria pilot were very low (e.g., less than 20 ppb). However, because of oil interference with the colorimetric-detection method, we could not state definitively that the produced dissolved-oxygen content was zero.

When polymer solutions that are laden with $Fe^{2+}$ enter the production well from the formation, they contain no dissolved oxygen. When this solution contacts atmospheric air, a tremendous

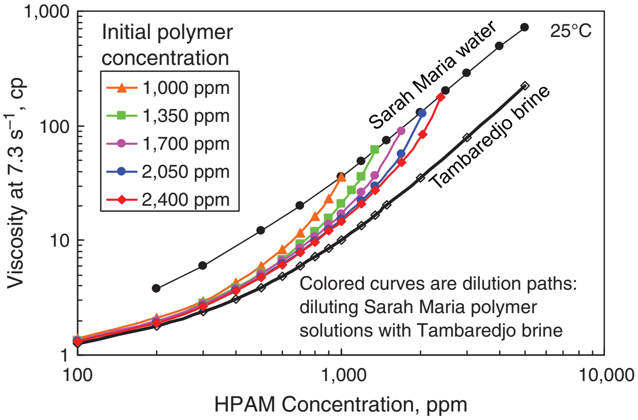

**Fig. 7—Viscosity vs. concentration at 7.3 $s^{-1}$ and 25°C.**

**TABLE 4—COMPARISON OF VISCOSITIES (7.3 $s^{-1}$, 25°C) IN SARAH MARIA VS. TAMBAREDJO WATERS**

| Polymer Concentration (ppm) | Viscosity in Sarah Maria Water (cp) | Viscosity in Tambaredjo Brine (cp) | Viscosity Ratio |
|---|---|---|---|
| 5,000 | 714 | 223 | 3.2 |
| 3,000 | 288 | 78.2 | 3.7 |
| 2,000 | 131 | 35.3 | 3.7 |
| 1,500 | 74.9 | 20.4 | 3.7 |
| 1,200 | 49.4 | 13.6 | 3.6 |
| 1,000 | 35.7 | 10.1 | 3.5 |
| 700 | 19.8 | 6.0 | 3.3 |
| 500 | 12.2 | 3.9 | 3.1 |
| 300 | 6.0 | 2.4 | 2.5 |
| 200 | 3.8 | 1.8 | 2.1 |

abundance of oxygen is available to react with and substantially degrade the HPAM polymer. Put another way, the ratio of available free oxygen (in the air) to the polymer (i.e., the small amount in a sample cylinder) is very large. Contact with the atmosphere continually replenishes any dissolved oxygen that reacts with polymer in solution. In contrast, when a polymer solution is injected, the ratio of free oxygen to polymer is very small. The only free oxygen that is available to react with the polymer is that 3,000 to 8,000 ppb that was dissolved in the water at surface conditions. (Free air is not injected into the formation.) If 8 ppm (8,000 ppb) of oxygen destroys 8 ppm of polymer (out of 1,000 ppm polymer), the resultant viscosity loss is minor. Once the injected dissolved oxygen is consumed, it is not replenished. More-detailed discussion of HPAM degradation in the presense of iron and oxygen can be found in Shupe (1981); Yang and Treiber (1985); and Seright et al. (2010).

Our results may help explain the inconsistency between good production responses vs. highly degraded polymer observed in many past field projects. In particular, the Daqing polymer flood is by far the largest polymer flood in the world. This project has well-documented incremental oil recoveries of 12 to 20% of OOIP, with more than 200,000-BOPD incremental production as a result of polymer flooding (Wang et al. 2011; Wang et al. 2006)—in spite of observing 80 to 92% loss of polymer molecular weight upon transit through the reservoir (Zhang 1995; Wang et al. 2006; You et al. 2007).

## Dilution of Sarah Maria HPAM Solutions by Tambaredjo Brine

At the Sarah Maria polymer pilot, low-salinity Sarah Maria water is used to dissolve the HPAM. After this polymer solution is injected, it will mix to some degree with the resident Tambaredjo brine, which has a salinity of 9 to 10 times greater than the Sarah Maria source water (4700 vs. 500 ppm TDS). For a given concentration, HPAM polymers are known to provide much lower viscosities as salinity increases (Martin 1975). Divalent ions affect viscosity substantially more than monovalent cations. These facts raise concerns about how much viscosity loss will occur, as a function of the degree of mixing of Sarah Maria polymer solutions with Tambaredjo brine, and how much in-situ mixing occurs during the Sarah Maria polymer flood.

**How Much Viscosity Loss Will Occur, as a Function of the Degree of Mixing?.** On the basis of a field-water analysis, we prepared a synthetic version of the Sarah Maria source water that contained 200 ppm magnesium sulfate ($MgSO_4$), 120 ppm sodium sulfate ($Na_2SO_4$), 100 ppm sodium chloride (NaCl), and 80 ppm calcium chloride ($CaCl_2$). We also prepared a synthetic version of the Tambaredjo brine with 3,950 ppm NaCl, 400 ppm $MgCl_2$, and 350 ppm $CaCl_2$. Both fluids were filtered through 0.45-$\mu$m filters before addition of polymer. A polymer solution was prepared for each fluid using HPAM concentrations from 200 to 5,000 ppm. The 3630S HPAM was taken from the Sarah Maria pilot site (July 2012). For each solution, viscosity measurements were made as a function of shear rate at 25°C using an Anton Paar MCR301 rheometer with CC27-SN29031; $d = 0$ mm measuring system (concentric cylinder). Our experience has shown that viscosities measured with this rheometer match well with those from the Brookfield viscometer with the UL adapter. However, the MCR301 rheometer can measure torque values over a considerably broader range.

**Fig. 7** plots viscosity (at 7.3 $s^{-1}$ and 25°C) vs. polymer concentration in the Sarah Maria source water (solid circles) and in the Tambaredjo brine (open diamonds). For polymer concentrations greater than 1,000 ppm, the relation between viscosity ($\mu$, in cp) and concentration ($C$, in ppm) is described well by Eq. 1 in Sarah Maria source water and by Eq. 2 in Tambaredjo brine. **Table 4** reveals that for much of the concentration range for a given polymer concentration, the viscosity (at 7.3 $s^{-1}$) was approximately 3.6 times greater in the Sarah Maria water than in the Tambaredjo brine.

$$\mu_{\text{sarah maria}} = 10^{-4}C^{1.8575} \quad \ldots\ldots\ldots\ldots\ldots\ldots\ldots\ldots (1)$$

and

$$\mu_{\text{tambaredjo}} = 10^{-5}C^{1.9671}. \quad \ldots\ldots\ldots\ldots\ldots\ldots\ldots\ldots (2)$$

For five polymer solutions in Sarah Maria water (1,000 ppm, 1,350 ppm, 1,700 ppm, 2,050 ppm, and 2,400 ppm HPAM), we made dilutions with Tambaredjo brine and measured viscosities (Fig. 7). The dilution path for 1,000 ppm HPAM is described well (correlation coefficient: 0.9991) using Eq. 3, while the dilution path for 1,350 ppm HPAM is described well (correlation coefficient: 0.9978) using Eq. 4. The dilution path for 1,700 ppm HPAM is described well (correlation coefficient: 0.9928) using Eq. 5, although the fit prediction is 16% too high at 100 ppm polymer. The dilution path for 2,050 ppm HPAM is described moderately well (correlation coefficient: 0.9882) using Eq. 6, although the fit prediction is 24% too high at 100 ppm polymer and a few percent low for concentrations between 400 and 1,200 ppm. The dilution path for 2,400 ppm HPAM is described (correlation coefficient: 0.9831) using Eq. 7; the fit prediction is 36% too high at 100 ppm polymer, and typically 10% low for concentrations between 500 and 1,000 ppm.

$$\mu_{1000} = 1.0151e^{0.0035C}. \quad \ldots\ldots\ldots\ldots\ldots\ldots\ldots\ldots (3)$$

$$\mu_{1350} = 1.1243e^{0.0029C}. \quad \ldots\ldots\ldots\ldots\ldots\ldots\ldots\ldots (4)$$

$$\mu_{1700} = 1.3035e^{0.0025C}. \quad \ldots\ldots\ldots\ldots\ldots\ldots\ldots\ldots (5)$$

$$\mu_{2050} = 1.4216e^{0.0023C}. \quad \ldots\ldots\ldots\ldots\ldots\ldots\ldots\ldots (6)$$

$$\mu_{2400} = 1.6045e^{0.0020C}. \quad \ldots\ldots\ldots\ldots\ldots\ldots\ldots\ldots (7)$$

TABLE 5—VISCOSITIES (cp at 7.3 $s^{-1}$, 25°C) MEASURED AT VARIOUS POINTS ALONG THE DILUTION PATHS

| HPAM Concentration (ppm) | Viscosity in Sarah Maria Water (cp) | Viscosity (cp) Along Dilution Path, Starting at Given HPAM Concentration (ppm) | | | | | Viscosity in Tambaredjo Brine (cp) |
|---|---|---|---|---|---|---|---|
| | | 1,000 | 1,350 | 1,700 | 2,050 | 2,400 | |
| 2,400 | 177 | | | | | 177 | 44.6 |
| 2,050 | 127 | | | | 127 | 84.9 | 32.7 |
| 1,700 | 89.5 | | | 89.5 | 56.6 | 47.8 | 22.6 |
| 1,350 | 61.1 | | 61.1 | 36.2 | 29.8 | 27.2 | 16.5 |
| 1,000 | 35.7 | 35.7 | 21.0 | 17.0 | 15.4 | 14.6 | 10.1 |
| 700 | 19.8 | 11.6 | 9.2 | 8.5 | 7.8 | 7.8 | 6.0 |
| 500 | 12.2 | 6.0 | 5.2 | 5.1 | 4.8 | 4.8 | 3.9 |
| 300 | 6.0 | 2.9 | 2.8 | 2.8 | 2.7 | 2.6 | 2.4 |
| 200 | 3.8 | 2.1 | 2.0 | 2.0 | 1.9 | 1.9 | 1.8 |

**Table 5** compares viscosities measured at various points along the dilution paths. **Table 6** provides the resultant salinities upon mixing for the solutions described in Table 5.

**How Much In-Situ Mixing Occurs During the Sarah Maria Polymer Flood?** An important principle of polymer flooding is that a very efficient (piston-like) displacement of a reservoir can occur if the injected-polymer viscosity is as large as the product of waterflood mobility ratio times the permeability contrast (Wang et al. 2006; Seright 2010). For that case, minimum mixing should occur between the injected polymer solution and the displaced water. At Sarah Maria, given an endpoint mobility ratio of 0.07, an oil viscosity of 600 cp, and a permeability contrast of 10:1, the optimum injected viscosity could be 420 cp. For injected viscosities less than this value, some level of mixing should be expected for the polymer solution and the formation water.

**What Factors Promote In-Situ Mixing and Salinity Increase?** At least three factors promote mixing of aqueous fluids in the formation and increased salinity for the polymer bank—crossflow, ion exchange, and diffusion/dispersion. We note that the water cut for the pilot averaged approximately 50% well before water or polymer injection began. Because no active waterdrive was present at this time, the consensus is that mobile water had been present since discovery of the field. Accepted reservoir engineering (Craig 1971) indicates that mobile and connate water should be displaced efficiently, without much mixing if that water exists in the most-permeable pathway. However, if crossflow can occur, polymer solution that crossflows into the less-permeable zones can have a large area of contact with saline water in the less-permeable zones, and therefore mixing could occur.

Ion exchange from formation clays can also increase salinity of low-salinity polymer solutions. While in contact with the resident-formation brine, existing clays may be heavily loaded with ions, especially calcium and magnesium. Those ions will be released into the low-salinity polymer bank when it passes (Lake 1989).

Diffusion/dispersion is a third factor that promotes mixing and salinity increase in the polymer bank. The dispersion process is associated with convective mixing during flow, and the crossflow phenomenon mentioned in the preceding paragraphs is a part of this process. The dispersivity ($\alpha$) in reservoirs has been suggested to be (roughly) proportional to the distance travelled by the injected bank (Arya et al. 1988). Diffusion is a relatively slow process that is proportional to the square root of time of contact between the polymer bank and the displaced brine bank (Lake 1989; Seright 1991a).

**How Much Did the Salinity of the Polymer Bank Actually Increase?** Fig. 2 indicates produced-water salinities (during polymer flooding) that dropped to 1,100 ppm TDS in Well 1N11 and to 2,000 ppm TDS in Wells 1N06 and 1N01. In February 2012, analysis revealed HPAM concentrations of approximately 700 ppm in Well 1N11, 350 ppm in Well 1N06, and 380 ppm in Well 1N01. Assume that the polymer concentration reflects the contribution of the production that comes from a polymer injector (injecting 1,000 ppm HPAM). So in Well 1N11, the polymer was diluted from 1,000 ppm to 700 ppm. If the injected water had 500-ppm-TDS salinity, an equivalent dilution with 4,700-ppm-TDS Tambaredjo brine should result in a produced salinity of 1,800 ppm TDS. Instead, a salinity of approximately 1,100 ppm TDS was observed. Polymer retention retards polymer propagation relative to brine in porous media. This fact may explain why our produced salinities were less than expected from simple mixing arguments.

For Wells 1N06 and 1N01, the polymer was diluted from 1,000 ppm to approximately 350 ppm. If the injected water had

TABLE 6—SALINITIES (ppm TDS) AT VARIOUS POINTS ALONG THE DILUTION PATHS FOR TABLE 5

| HPAM Concentration (ppm) | Sarah Maria Salinity (ppm TDS) | Salinity (ppm TDS) Along Dilution Path, Starting at Given HPAM Concentration (ppm) | | | | | Tambaredjo Salinity (ppm TDS) |
|---|---|---|---|---|---|---|---|
| | | 1,000 | 1,350 | 1,700 | 2,050 | 2,400 | |
| 2,400 | 500 | | | | | 500 | 4,700 |
| 2,050 | 500 | | | | 500 | 1,113 | 4,700 |
| 1,700 | 500 | | | 500 | 1,217 | 1,725 | 4,700 |
| 1,350 | 500 | | 500 | 1,365 | 1,934 | 2,338 | 4,700 |
| 1,000 | 500 | 500 | 1,589 | 2,229 | 2,651 | 2,950 | 4,700 |
| 700 | 500 | 1,760 | 2,522 | 2,971 | 3,266 | 3,475 | 4,700 |
| 500 | 500 | 2,600 | 3,144 | 3,465 | 3,676 | 3,825 | 4,700 |
| 300 | 500 | 3,440 | 3,767 | 3,959 | 4,085 | 4,175 | 4,700 |
| 200 | 500 | 3,860 | 4,078 | 4,206 | 4,290 | 4,350 | 4,700 |

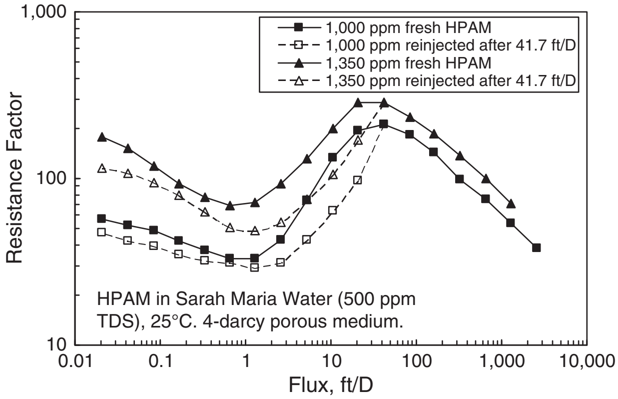

**Fig. 8—Resistance factor vs. flux for HPAM in Sarah Maria water.**

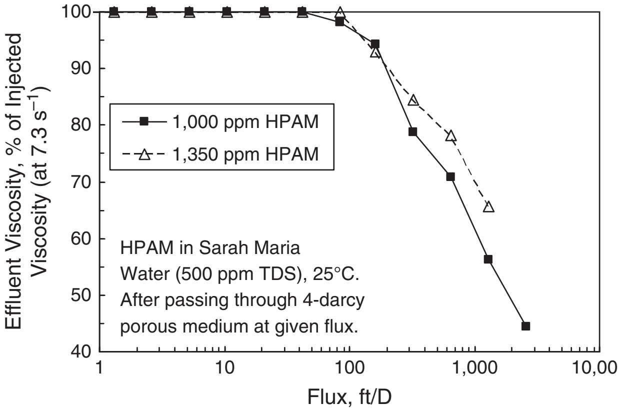

**Fig. 9—Viscosities of solutions after being forced through the core at a given flux.**

500-ppm-TDS salinity, an equivalent dilution with 4,700-ppm-TDS Tambaredjo brine should result in a produced salinity of 3,230 ppm TDS. Instead, a salinity of approximately 2,000 ppm TDS was observed. Because the observed salinity of the produced water was less than expected, it is suggested that the in-situ-mixing mechanisms mentioned in the preceding subsections (crossflow, ion exchange, dispersion/diffusion) were not as active as we might have feared. It suggests that the polymer banks may retain low salinity and therefore high viscosity for much of the way through the pattern.

## Rheology in Porous Media, Mechanical Degradation, and Injectivity

**Rheology and Mechanical Degradation.** In this subsection, we consider whether the polymer was expected to experience mechanical degradation during injection. Results from this analysis impact our conclusions about injectivity and the presence of near-wellbore fractures in the injection wells. Rheology in porous media and mechanical degradation are directly related to the fluid velocity or flux in porous media (Maerker 1975; Seright et al. 2009; Seright et al. 2011). Consequently, using the methods described in Seright et al. (2011), we determined rheology in a 4-darcy porous medium for the two polymer concentrations that have been used at the Sarah Maria pilot: 1,000 ppm HPAM in Sarah Maria water (500 ppm TDS) and 1,350 ppm HPAM in Sarah Maria water. **Fig. 8** plots resistance factor vs. flux for these solutions. (Resistance factor is the effective viscosity in porous media, relative to water. See Jennings et al. 1971 or Seright et al. 2011.) **Fig. 9** plots viscosity (measured at 7.3 s$^{-1}$ and 25°C, and expressed as a percentage of the injected polymer-solution viscosity) for the effluent vs. flux at which the polymer solution was forced through the core.

Fig. 8 was generated as follows. First, the core was saturated with Sarah Maria water, and porosity and permeability were determined. Next, we injected freshly prepared 1,000 ppm 3630S (in Sarah Maria water) at high flux (2,609 ft/D) and measured the stabilized resistance factor in the second section of the core (the core had one internal pressure tap, to eliminate end effects associated with the inlet face. See Seright et al. 2009). Then we halved the injection rate and allowed pressures to stabilize and resistance factor to be determined again. This process was repeated in stages to determine the resistance factors associated with the solid squares in Fig. 8. Between 2,609 and 41.7 ft/D, the resistance factor appeared to increase with decreasing flux. However, this behavior was not shear thinning. For each flux between 41.7 and 2,609 ft/D, the polymer was mechanically degraded to a different extent, as demonstrated by the solid squares in Fig. 9.

As flux was lowered from 41.7 to 1 ft/D, resistance factor decreased dramatically (by a factor of 6.4 for the 1,000-ppm case) with decreasing flux (Fig. 8) and little or no mechanical degradation occurred (Fig. 9). This behavior has been consistently reported by experimentalists in the literature for the past 40 years (Jennings et al. 1971; Maerker 1975; Heemskerk et al. 1984; Seright 1991b; Seright et al. 2011). Oddly, a misconception persists that HPAM solutions show only Newtonian or shear-thinning behavior in porous media—not shear thickening (Lake 1989). Shear thickening in porous media has been attributed to increased stresses and energy expenditure associated with disentanglement and elongation of coiled HPAM molecules as they flow through the sequentially contracting/dilating flow paths within porous media. Previous studies of this shear-thickening behavior in porous media focused on solutions with salinities ranging from 3,000 ppm to 50,000 ppm TDS (Jennings et al. 1971; Maerker 1975; Heemskerk et al. 1984; Seright 1991b; Seright et al. 2011). Our study extends conditions in which this behavior has been observed down to only 500 ppm TDS.

For fluxes lower than 1 ft/D, shear thinning was seen as resistance factor increased with decreasing flux. If the salinity had been greater (than 500 ppm TDS), Newtonian or near-Newtonian behavior would have been seen in this flux range, depending on polymer concentration and molecular weight (Seright et al. 2009; Seright et al. 2011).

Next, we forced fresh 1,000-ppm 3630S through the core at 41.7 ft/D and collected the effluent. This flux (approximately 40 ft/D) is the condition that the polymer would have experienced at the Sarah Maria pilot if the completion was openhole, 8-in. in diameter, 300 B/D, and 10-ft formation height (and no fracture was present). The effluent from this experiment was reinjected using a series of lower rates to obtain the open squares in Fig. 8. Note that only shear-thickening behavior is seen between 41.7 and 1 ft/D. Below 1 ft/D, some shear thinning is seen.

Next, we repeated these steps with 1,350 ppm 3630S to obtain the solid triangles (for fresh HPAM) and the open triangles (for polymer that had previously experienced 41.7 ft/D, as at the injection face for an openhole completion) in Fig. 8. A key conclusion from Fig. 9 was that mechanical degradation was expected to be small (for the actual injection condition of 300 B/D)—even if the completion was openhole (and sandface flux was approximately 40 ft/D). As will be demonstrated next, the injection wells actually have open fractures during polymer injection—thus creating a much greater area to flow and minimizing mechanical degradation.

**Injectivity.** The open squares and open triangles in Fig. 8 are the relevant curves if we want to estimate injectivity for these solutions. These curves were entered (along with field-injection conditions) to calculate injectivity (relative to water) for unfractured vertical wells with radial flow. (The method is described in Seright et al. 2009.) **Fig. 10** shows the injectivity predictions as a function of polymer penetration away from the well. This figure clearly shows that if flow is radial for vertical openhole injection wells (with no fractures), injectivity should be dramatically less

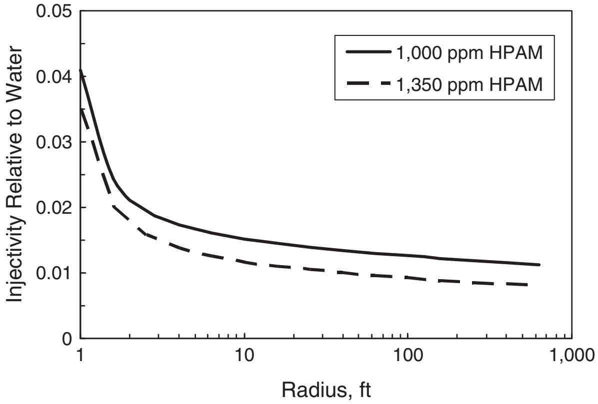

**Fig. 10—Injectivity predictions assuming unfractured openhole vertical Sarah Maria injectors.**

for polymer solutions than for water. Specifically, polymer-solution injectivity should be only 1 to 2% of that for water.

The results in Fig. 10 can be appreciated on a simpler level by realizing that resistance factors for the dashed curves in Fig. 8 never fall below 29 for 1,000 ppm HPAM and 49 for 1,350 ppm HPAM. If flow is truly radial away from the injector (as in an openhole completion with no fracture), injectivity (relative to water) for a Newtonian fluid can be estimated by

$$I/I_o = \ln(r_e/r_w)/[F_r \ln(r_p/r_w) + \ln(r_e/r_p)]. \quad \ldots\ldots\ldots \quad (8)$$

In this equation, $r_p$ is the radius of the polymer front, $F_r$ is the resistance factor (minimum of 29 and 49 in our cases), $r_e$ is the external drainage radius, and $r_w$ is the wellbore radius. A few calculations with this equation reveal that for even small polymer-front radii, the injectivity is predicted to fall rapidly to less than 4% of the water injectivity (i.e., 1/29) for the 1,000 ppm polymer and to 2% (i.e., 1/49) for the 1,350 ppm polymer. The actual injectivity losses will be greater because the actual resistance factors will be greater (than 29 or 49) for the vast majority of the flow field.

How do the predictions from Fig. 10 compare with the observed injectivity behavior in the Sarah Maria polymer-flood pilot? Consider Injection Well 1M101 in August 2008. As shown in **Table 7,** water was injected first at a low rate (100 B/D), resulting in a downhole pressure of 553 psi and an injectivity of 0.28 (B/D)/psi. When the rate was increased to 650 B/D, the injectivity rate more than tripled to 1.01 (B/D)/psi, indicating that a fracture was open at the high rate. When the water rate was reduced to 125 B/D, the injectivity decreased to 0.44 (B/D)/psi, suggesting that the fracture closed substantially. When the rate was increased again to 650 B/D, injectivity tripled to 1.21 (B/D)/psi, indicating a reopening of the fracture. Reducing the water rate again to 175 B/D decreased injectivity to 0.65 (B/D)/psi, indicating at least partial fracture closure. When water rate was increased a third time to 650 B/D, injectivity increased to 1.48 (B/D)/psi, indicating fracture reopening. Thus, the process of opening and closing the fracture was at least partially reversible. Because this was the first time that water had been injected into this well, it seems likely that injectivity should increase with increased water-injection volume, because low-viscosity water displaced some viscous oil away from the wellbore. Also, note that for this last water-injection step, the downhole pressure was 638 psi—well below the accepted formation-parting pressure of 800 psi—and yet the fracture was obviously open.

Finally, in Table 7, note that 1,000 ppm polymer solution was injected at 175 B/D, resulting in a downhole pressure of 635 psi and an injectivity of 0.40 (B/D)/psi. Let us assume that the fracture was closed during the previous water injection at 175 B/D, in which injectivity was 0.65 (B/D)/psi. If no fractures are open, the expected injectivity during injection of 1,000 ppm HPAM (from Fig. 10) would be reduced to approximately 1% of that of water, or approximately 0.0065 (B/D)/psi. Instead, the observed injectivity was 0.40 (B/D)/psi, or approximately 61 times greater than expected. Thus, a fracture was open during polymer injection.

**TABLE 7—INJECTIVITY TEST OF AUGUST 2008, IN WELL 1M101**

| Injectant | Injection Rate (B/D) | BHP (psi) | Injectivity [(B/D)/psi] |
|---|---|---|---|
| water | 100 | 553 | 0.28 |
| water | 650 | 845 | 1.01 |
| water | 125 | 482 | 0.44 |
| water | 650 | 737 | 1.21 |
| water | 175 | 471 | 0.65 |
| water | 650 | 638 | 1.48 |
| 1,000 ppm polymer | 175 | 635 | 0.40 |

A similar observation was found for the second injector, Well 1N062, in May 2010. Water was injected first at 343 B/D, resulting in a downhole pressure of 488 psi and an injectivity of 1.19 (B/D)/psi. When the rate was increased to 685 B/D, the downhole pressure increased to 638 psi and injectivity increased to 1.56 (B/D)/psi. This 31% injectivity increase might indicate fracture opening, but the point is debatable. However, when 1,000 ppm polymer solution was injected at 343 B/D, the downhole pressure was 744 psi and injectivity was 0.63 (B/D)/psi. If no fractures were open, the expected injectivity for polymer solution should have been approximately 0.012 (B/D)/psi. The actual polymer injectivity was approximately 52 times greater than expected. So again, the fracture was open during polymer injection.

Previous work (Gadde and Sharma 2001; Seright et al. 2009) indicates that once fractures are opened, the fracture area increases to accommodate increased injection rate or increased injectant viscosity—with small increases in downhole pressure. This concept can be used to make a rough estimate of the open-fracture area and the extent of the fracture. For example, if the injectivity is 61 times greater than expected for injection into an openhole completion, the fracture area is roughly 61 times greater than that associated with the open hole. Because the openhole area is approximately 42 $\text{ft}^2$ for our wells, the implied area during polymer injection is 2,562 $\text{ft}^2$. Given the depth of the Tambaredjo formation (1,000 ft) and the local stress field, induced fractures are horizontal. Thus, a fracture area of 2,562 $\text{ft}^2$ translates to a horizontal fracture (with an upper and lower face) that extends 20 ft from the well. This short fracture does not jeopardize sweep (i.e., create severe channeling) because the nearest production well is more than 300 ft away. This point is consistent with our observation that severe channeling did not occur during the Sarah Maria polymer pilot (Moe Soe Let et al. 2012). However, the fracture increases injectivity tremendously for the polymer solution. The fracture also reduced the possibility of HPAM mechanical degradation. By increasing the sandface area by a factor of 61, the velocity when the polymer enters the formation is reduced in proportion.

## Conclusions

1. Two new methods were developed for anaerobically sampling polymer solutions from production wells in the Sarah Maria polymer-flood-pilot project in Suriname. Whereas previous methods indicated severe polymer degradation, the improved methods revealed that the polymer propagated intact more than 300 ft through the Tambaredjo formation. Our results may help explain the inconsistency between good production responses vs. highly degraded polymer observed in many past field projects.
2. Our work demonstrating HPAM stability focused on the reservoir temperature of 38°C. Previous field applications that observed severe polymer degradation may benefit from re-examination of produced-polymer samples by use of our methods. Expanded application of these methods may help clarify

the limiting conditions (especially temperature limits) for polymer flooding.

3. Both of our new sampling methods can be effective if applied properly. Sampling Method 1 may be preferred for the first application in a field if previous methods indicated severe polymer degradation. It may also be preferred if only one well is tested at a time. Method 2 may be preferred if the operater wishes to collect samples from multiple wells before returning to the laboratory for analysis.
4. Analysis of produced salinity, polymer concentration, and viscosity indicated that the polymer banks retained low salinity and therefore high viscosity for much of the way through the Sarah Maria polymer-flood-pilot pattern.
5. A strong shear-thickening rheology was observed for 1,000 ppm and 1,350 ppm HPAM solutions in porous media, even though the salinity was only 500 ppm TDS. Injectivity analysis revealed that these solutions were injected above the formation parting pressure in the Sarah Maria polymer-injection wells.
6. Injectivity was insufficient until fractures were initiated hydraulically; however, the fractures propagated only approximately 20 ft and did not jeopardize sweep efficiency. In contrast, the short fractures greatly improved polymer injectivity and reduced concern about polymer mechanical degradation.

## Nomenclature

$C$ = polymer concentration, ppm (mg/L)
$F_r$ = polymer-solution resistance factor (brine mobility divided by polymer-solution mobility)
$I/I_o$ = injectivity relative to water
$r_e$ = external drainage radius, ft (m)
$r_p$ = radius of polymer penetration, ft (m)
$r_w$ = wellbore radius, ft (m)
$\alpha$ = dispersivity, ft (m)
$\mu$ = viscosity, cp (mPa·s)

## References

Arya, A., Hewett, T.A., Larson, R.G. et al. 1988. Dispersion and Reservoir Heterogeneity. *SPE Res Eng* **3** (1): 139–148. SPE-14364-PA. http://dx.doi.org/10.2118/14364-PA.

Craig, F.F. Jr. 1971. *The Reservoir Engineering Aspects of Waterflooding*, Vol. 3, 45–75. Richardson, Texas: Monograph Series, SPE.

Gadde, P.B. and Sharma, M.M. 2001. Growing Injection Well Fractures and Their Impact on Waterflood Performance. Presented at the SPE Annual Technical Conference and Exhibition, New Orleans, 30 September–3 October. SPE-71614-MS. http://dx.doi.org/10.2118/71614-MS.

Heemskerk, J., Rosmalen, R., Janssen-van, R. et al. 1984. Quantification of Viscoelastic Effects of Polyacrylamide Solutions. Presented at the SPE Enhanced Oil Recovery Symposium, Tulsa, 15–18 April. SPE-12652-MS. http://dx.doi.org/10.2118/12652-MS.

Jennings, R.R., Rogers, J.H., and West, T.J. 1971. Factors Influencing Mobility Control by Polymer Solutions. *J Pet Technol* **23** (3): 391–401. SPE-2867-PA. http://dx.doi.org/10.2118/2867-PA.

Lake, L.W. 1989. *Enhanced Oil Recovery*, 323–234, 396–400. Englewood Cliffs, New Jersey: Prentice Hall.

Maerker, J.M. 1975. Shear Degradation of Partially Hydrolyzed Polyacrylamide Solutions. *SPE J.* **15** (4): 311–322. SPE-5101-PA. http://dx.doi.org/10.2118/5101-PA.

Maitin, B.K. 1992. Performance Analysis of Several Polyacrylamide Floods in North German Oil Fields. Presented at the SPE/DOE Enhanced Oil Recovery Symposium, Tulsa, 22–24 April. SPE-24118-MS. http://dx.doi.org/10.2118/24118-MS.

Martin, F.D. 1975. The Effect of Hyrolysis of Polyacrylamide on Solution viscosity, Polymer Retention and Flow Resistance Properties. Presented at the SPE Rocky Mountain Regional Meeting, Denver, 7–9 April. SPE-5339-MS. http://dx.doi.org/10.2118/5339-MS.

Moe Soe Let, K.P., Manichand, R.N., and Seright, R.S. 2012. Polymer Flooding a ~500-cp Oil. Presented at the SPE Improved Oil Recovery Symposium, Tulsa, 14–18 April. SPE-154567-MS. http://dx.doi.org/10.2118/154567-MS.

Moradi-Araghi, A. and Doe, P.H. 1987. Hydrolysis and Precipitation of Polyacrylamides in Hard Brines at Elevated Temperatures. *SPE Res Eng* **2** (2): 189–198. SPE-13033-PA. http://dx.doi.org/10.2118/13033-PA.

Putz, A.G., Bazin, B., and Pedron, B.M. 1994. Commercial Polymer Injection in the Courtenay Field, 1994 Update. Presented at the SPE Annual Technical Conference and Exhibition, New Orleans, 25–28 September. SPE-28601-MS. http://dx.doi.org/10.2118/28601-MS.

Seright, R.S. 1991a. Impact of Dispersion on Gel Placement for Profile Control. *SPE Res Eng* **6** (3): 343–352. SPE-20127-PA. http://dx.doi.org/10.2118/20127-PA.

Seright, R.S. 1991b. Effect of Rheology on Gel Placement. *SPE Res Eng* **6** (2): 212–218. SPE-18502-PA. http://dx.doi.org/10.2118/18502-PA.

Seright, R.S., Seheult, M., Kelco, C.P. et al. 2009. Injectivity Characteristics of EOR Polymers. *SPE Res Eval & Eng* **12** (5): 783–792. SPE-115142-PA. http://dx.doi.org/10.2118/115142-PA.

Seright, R.S., Campbell, A.R., Mozley, P.S. et al. 2010. Stability of Partially Hydrolyzed Polyacrylamides at Elevated Temperatures in the Absence of Divalent Cations. *SPE J.* **15** (2): 341–348. SPE-121460-PA. http://dx.doi.org/10.2118/121460-PA.

Seright, R. 2010. Potential for Polymer Flooding Reservoirs With Viscous Oils. *SPE Res Eval & Eng* **13** (4): 730–740. SPE-129899-PA. http://dx.doi.org/10.2118/129899-PA.

Seright, R.S., Fan, T., Wavrik, K. et al. 2011. New Insights Into Polymer Rheology in Porous Media. *SPE J.* **16** (1): 35–42. SPE-129200-PA. http://dx.doi.org/10.2118/129200-PA.

Shupe, R.D. 1981. Chemical Stability of Polyacrylamide Polymers. *J Pet Technol* **33** (8): 1513–1529. SPE-9299-PA. http://dx.doi.org/10.2118/9299-PA.

Wang, D., Wang, G., Xia, H. et al. 2011. Incremental Recoveries in the Field of Large Scale High Viscous-Elastic Fluid Flooding are Double that of Conventional Polymer Flooding. Presented at the SPE Annual Technical Conference and Exhibition, Denver, 30 October–2 November. SPE-146473-MS. http://dx.doi.org/10.2118/146473-MS.

Wang, D., Han, P., Shao, Z. et al. 2006. Sweep Improvement Options for the Daqing Oil Field. Presented at the SPE/DOE Symposium on Improved Oil Recovery, Tulsa, 22–26 April. SPE-99441-MS. http://dx.doi.org/10.2118/99441-MS.

Yang, S.H. and Treiber, L.E. 1985. Chemical Stability of Polyacrylamide Under Simulated Field Conditions. Presented at the SPE Annual Technical Conference and Exhibition, Las Vegas, Nevada, USA, 22–26 September. SPE-14232-MS. http://dx.doi.org/10.2118/14232-MS.

You, Q., Zhao, F.L., Wang, Y.F. et al. 2007. Comparison of the Properties of Injected and Released Polyacrylamide in Polymer Flooding. *Journal of Beijing University of Chemical Technology* **34** (4): 414–417.

Zhang, J. 1995. *The EOR Technology*. Beijing: Petroleum Industry Publishing Company of China.

## SI Metric Conversion Factors

| | |
|---|---|
| cp × 1.0* | E−03 = Pa·s |
| ft × 3.048* | E−01 = m |
| in. × 2.54* | E+00 = cm |
| md × 9.869 233 | E−04 = $\mu m^2$ |
| psi × 6.894 757 | E+00 = kPa |

*Conversion factor is exact.

**Renuka N. Manichand** is an enhanced-oil-recovery (EOR) project engineer with Staatsolie Maatschappij Suriname N.V. in the Republic of Suriname, South America. She has contributed to a reservoir-characterization study and the implementation, execution, and evaluation of a polymer-flooding field pilot in the Tambaredjo field, Suriname. Manichand has authored/coauthored three SPE papers related to this EOR field pilot. She holds a BS degree and an MS degree in chemical engineering and a PhD degree in chemistry from the Federal University of Rio Grande do Norte, Brazil.

**Kathleen Moe Soe Let** is the EOR team leader with Staatsolie Maatschappij Suriname N.V. in Suriname. She has worked for

Staatsolie for more than 10 years, with experience in reservoir engineering and reservoir management, and has been responsible for the EOR projects within Staatsolie for the past 3 years. Moe Soe Let holds a BS degree in mining, a post-graduate degree in petroleum techniques, and an MS degree in petroleum geology.

**Ludwig Gil** is a research-and-development (R&D) project engineer with SNF. He joined SNF in 2003. Mainly specializing in water treatment, he has participated in several EOR project startups in South America, the Middle East, and Europe, and he is a coholder of two patents. Gil holds an MS degree in process engineering and environmental science from Chalmers University.

**Bernard Quillien** is an R&D project leader with SNF. He joined SNF in 1993 and is primarily in charge of oilfield laboratory applications, specializing in fluid mechanics. Quillien has also served as laboratory manager in charge of many EOR project startups in South America, the Middle East, Europe, and Asia. Previously, he worked for Dowell Schlumberger in well cementing and drilling fluids. Quillien is a coholder of one patent, and has coauthored three SPE papers. He holds a degree in chemistry from Rennes University.

**Randy Seright** is a senior engineer at the Petroleum Recovery Research Center of New Mexico Institute of Mining and Technology in Socorro, New Mexico, where he has worked for the past 26 years. He has been a registered professional engineer since 1983. Seright holds a PhD degree in chemical engineering from the University of Wisconsin (Madison). He received the SPE/US Department of Energy IOR Pioneer award in 2008 for his work on using polymer and gels to improve oil recovery.